J|A|C|S
ARTICLES
Published on Web 10/26/2006

Oxidation of Nitrite by a *trans*-Dioxoruthenium(VI) Complex: Direct Evidence for Reversible Oxygen Atom Transfer

Wai-Lun Man,[†] William W. Y. Lam,[†] Wai-Yeung Wong,[‡] and Tai-Chu Lau*,[†]

Contribution from the Department of Biology and Chemistry, City University of Hong Kong, Tat Chee Avenue, Kowloon Tong, Hong Kong, China, and Department of Chemistry, Hong Kong Baptist University, Waterloo Road, Kowloon Tong, Hong Kong, China

Received July 13, 2006; E-mail: bhtclau@cityu.edu.hk

Abstract: Reaction of *trans*-$[Ru^{VI}(L)(O)_2]^{2+}$ (**1**, L = 1,12-dimethyl-3,4:9,10-dibenzo-1,12-diaza-5,8-dioxacyclopentadecane, a tetradentate macrocyclic ligand with N_2O_2 donor atoms) with nitrite in aqueous solution or in H_2O/CH_3CN produces the corresponding (nitrato)oxoruthenium(IV) species, *trans*-$[Ru^{IV}(L)(O)(ONO_2)]^+$ (**2**), which then undergoes relatively slow aquation to give *trans*-$[Ru^{IV}(L)(O)(OH_2)]^{2+}$. These processes have been monitored by both ESI/MS and UV/vis spectrophotometry. The structure of *trans*-$[Ru^{IV}(L)(O)(ONO_2)]^+$ (**2**) has been determined by X-ray crystallography. The ruthenium center adopts a distorted octahedral geometry with the oxo and the nitrato ligands trans to each other. The Ru=O distance is 1.735(3) Å, the $Ru-ONO_2$ distance is 2.163(4) Å, and the $Ru-O-NO_2$ angle is 138.46(35)°. Reaction of *trans*-$[Ru^{VI}(L)(^{18}O)_2]^{2+}$ (**1**-$^{18}O_2$) with $N^{16}O_2^-$ in H_2O/CH_3CN produces the ^{18}O-enriched (nitrato)oxoruthenium(IV) species **2**-$^{18}O_2$. Analysis of the ESI/MS spectrum of **2**-$^{18}O_2$ suggests that scrambling of the ^{18}O atoms has occurred. A mechanism that involves linkage isomerization of the nitrato ligand and reversible oxygen atom transfer is proposed.

Introduction

The interconversion between nitrite and nitrate (eq 1) is of fundamental interest and of biological importance.[1−3]

$$NO_3^- + 2H^+ + 2e^- \rightleftharpoons NO_2^- + H_2O \qquad (1)$$

The oxidation of nitrite to nitrate by a variety of substitution-inert one-electron oxidants proceeds initially by outer-sphere electron transfer, and a self-exchange rate constant of 0.3 M^{-1} s^{-1} for the NO_2/NO_2^- couple has been derived by using the Marcus cross-relation.[4−7] Oxidation of nitrite by a number of potential oxygen atom donors has also been reported.[8−14] In principle these reactions could occur by oxygen atom transfer (OAT); however, so far there has been no definite proof for such a direct process, despite its apparent simplicity. For example, the reaction between OCl^- and NO_2^-, which has long been regarded as one of the classic examples of an OAT process,[8] actually proceeds by Cl^+ transfer from HOCl to NO_2^-.[9] Oxidation of nitrite by bis(2-ethyl-2-hydroxybutyrato)oxochromium(V) proceeds by inner-sphere electron transfer.[12] In the oxidation by a (salen)chromium(V) oxo complex, an OAT mechanism was proposed, but no evidence was provided.[13] Oxidation by $(NH_3)_4(H_2O)RhOOH$ should occur by OAT, although this has not been confirmed by oxygen isotope labeling experiments.[14]

The reverse reaction, i.e., the reduction of nitrate to nitrite, by molybdenum[15−18] and tungsten[19] complexes has also attracted much interest, because of its relevance to the molybdenum-containing enzyme nitrate reductase.[1−3] For this process there is one direct proof of OAT; by means of ^{18}O-labeling, the bis(μ-hydroxo)bis[aqua(1,4,7-triazacyclononane)molybdenum(II)] 4+ cation is shown to incorporate oxygen atoms from nitrate rather than from solvent water.[16] The reduction of nitrate to nitrite by $Mo^{IV}O(L\text{-}NS_2)(DMF)$[18] (L-$NS_2$ = 2,6-bis(2,2-diphenyl-2-mecaptoethyl)pyridine(2−)) and by a bis(dithiolene)-tungsten(IV) complex[19] in CH_3CN also likely occur by OAT.

We report here a study of the oxidation of nitrite in aqueous solution and in H_2O/CH_3CN by a cationic *trans*-dioxoruthenium-

[†] City University of Hong Kong.
[‡] Hong Kong Baptist University.

(1) Kroneck, P. M. H.; Abt, D. J. In *Molybdenum and Tungsten: Their Roles in Biological Processes*; Sigel, H., Sigel, A., Eds.; Marcel Dekker: New York, 2002; Vol. 39, pp 369−403.
(2) Hille, R. *Chem. Rev.* **1996**, *96*, 2757−2816.
(3) Young, C. G. In *Biomimetic Oxidations Catalyzed by Transition Metal Complexes*; Meunier, B., Ed.; Imperial College Press: London, 2000; pp 415−459.
(4) Wilmarth, W. K.; Stanbury, D. M.; Byrd, J. E.; Po, H. N.; Chua, C.-P. *Coord. Chem. Rev.* **1983**, *51*, 155−179.
(5) Ram, M. S.; Stanbury, D. M. *J. Am. Chem. Soc.* **1984**, *106*, 8136−8142.
(6) Hoddenbagh, J. M. A.; Macartney, D. H. *Inorg. Chem.* **1990**, *29*, 245−251.
(7) deMaine, M. M.; Stanbury, D. M. *Inorg. Chem.* **1991**, *30*, 2104−2109.
(8) Anbar, M.; Taube, H. *J. Am. Chem. Soc.* **1958**, *80*, 1073−1077.
(9) Johnson, D. W.; Margerum, D. W. *Inorg. Chem.* **1991**, *30*, 4845−4851.
(10) Dozsa, L.; Szilassy, I.; Beck, M. T. *Inorg. Chim. Acta* **1977**, *23*, 29−34
(11) Durham, D. A.; Dozsa, L.; Beck, M. T. J. *Inorg. Nucl. Chem.* **1971**, *33*, 2971−2979.
(12) Ghosh, S. K.; Bose, R. N.; Gould, E. S. *Inorg. Chem.* **1987**, *26*, 2688−2692.
(13) Kanthimathi, M.; Nair, B. U. *Int. J. Chem. Kinet.* **2004**, *36*, 79−86.
(14) Lemma, K.; Bakac, A. *Inorg. Chem.* **2004**, *43*, 6224−6227.
(15) Holm, R. H. *Chem. Rev.* **1987**, *87*, 1401−1449 and references therein.
(16) Wieghardt, K.; Woeste, M.; Roy, P. S.; Chaudhuri, P. *J. Am. Chem. Soc.* **1985**, *107*, 8276−8277.
(17) Craig, J. A.; Holm, R. H. *J. Am. Chem. Soc.* **1989**, *111*, 2111−2115.
(18) Thapper, A.; Behrens, A.; Fryxelius, J.; Johansson, M. H.; Prestopino, F.; Czaun, M.; Rehder, D.; Nordlander, E. *Dalton Trans.* **2005**, 3566−3571.
(19) Jiang, J.; Holm, R. H. *Inorg. Chem.* **2005**, *44*, 1068−1072.

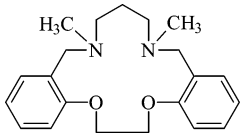

Figure 1. Structure of L.

(VI) complex, *trans*-$[Ru^{VI}(L)(O)_2]^{2+}$ (**1**) (L = 1,12-dimethyl-3,4:9,10-dibenzo-1,12-diaza-5,8- dioxacyclopentadecane, Figure 1), which was reported by Che.[20] The coordinated macrocyclic ligand L is resistant to oxidative degradation and ligand exchange. The oxidation of various organic and inorganic substrates by this complex has been reported.[20−25] Thermodynamic data ($E°$ vs NHE and pK_a values, 298 K) for the *trans*-$[Ru^{VI}(L)(O)_2]^{2+}$ system are summarized in Scheme 1.[20] At $[H^+]$ = 1.0 M, $E°$ for the NO_3^-/HNO_2 couple is 0.94 V.

Experimental Section

Materials. *trans*-$[Ru^{VI}(L)(O)_2](ClO_4)_2$ ([**1**]$(ClO_4)_2$) was prepared according to the literature.[20] Sodium nitrite was obtained from Riedel-deHaën and was recrystallized from water.[26] ^{18}O-labeled water (95% ^{18}O-enriched) was obtained from Isotec. Water for kinetic experiments was distilled twice from alkaline permanganate. Ionic strength was maintained with sodium trifluoroacetate.

Instrumentation. IR spectra were recorded as KBr pellets on a Nicolet Avatar 360 FT-IR spectrophotometer at 4 cm^{-1} resolution. Elemental analyses were done on an Elementar Vario EL analyzer. Magnetic measurement (solid sample, Gouy method) was performed at 20 °C using a Sherwood magnetic balance (Mark II). Ion chromatography was performed with a Wescan ICM 300 ion chromatograph equipped with an Alltech 335 suppressor module and an Alltech Allsep anion column. The mobile phase was 0.9 mM Na_2CO_3 and 0.9 mM $NaHCO_3$. Electrospray ionization mass spectra (ESI/MS) were obtained on a PE SCIEX API 365 mass spectrometer. The analyte solution was continuously infused with a syringe pump at a constant flow rate of 5 μL min^{-1} into the pneumatically assisted electrospray probe with nitrogen as the nebulizing gas. The declustering potential was typically set at 10−20 V.

Preparation of $[Ru^{IV}(L)(O)(ONO_2)](ClO_4)$ ([2]ClO_4). Solid $NaNO_2$ (4.5 mg, 0.065 mmol) was slowly added with stirring to an orange solution (2 mL) of $[Ru^{VI}(L)(O)_2](ClO_4)_2$ (40 mg, 0.060 mmol) in H_2O/CH_3CN (1:1, v/v). After 10 min the light purple solid was filtered out, washed with water (ca. 1 mL), and then dried in vacuo. Yield: 40%. Anal. Calcd for $C_{21}H_{28}N_3O_{10}ClRu$: C, 40.75; H, 4.56; N, 6.79. Found: C, 40.86; H, 4.58; N, 7.04. IR (KBr): ν(Ru=O) 835 cm^{-1}; $\nu_{sym}(NO_2)$ 1275 cm^{-1}; ν(N−O) 1015 cm^{-1}. UV/vis (CH_3CN) [λ_{max}, nm (ϵ, mol^{-1} dm^3 cm^{-1})]: 203 (36 900), 266 (5080), 557 (80), 665 sh (30). ESI/MS: m/z = 520, $[M]^+$. Magnetic measurement: μ_{eff} = 2.97 μ_B.

X-ray Crystallography. Crystals of [**2**]ClO_4 were obtained from CH_3CN/Et_2O. The data were collected on a Bruker Axs SMART 1000 CCD area-detector diffractometer using graphite-monochromated Mo Kα radiation (λ = 0.710 73 Å) at 293 K. Selected crystallographic data for [**2**]ClO_4: $C_{21}H_{28}ClN_3O_{10}Ru$, formula weight = 618.98; 0.25 × 0.22 × 0.14 mm; monoclinic, space group $P2_1/n$; a = 12.2758(12), b = 14.7281(14), c = 13.6554(13) Å; β = 104.4(1)°; V = 2391.29(40) Å^3; ρ_{calc} = 1.719 g cm^{-3}; Z = 4; $F(000)$ = 1264; total/independent reflections = 4206/3161; R_1/wR_2 = 0.0408/0.1092 for $I > 2\sigma(I)$; maximum/minimum transmission 0.9174/1.0000; GOF = 1.043; parameters = 325. The raw intensity data frames were integrated with the SAINT+ program using a narrow-frame integration algorithm.[27] Corrections for Lorentz and polarization effects were also applied by SAINT. For each analysis, an empirical absorption correction based on the multiple measurement of equivalent reflections was applied by using the program SADABS.[28] The structure was solved by direct methods and expanded by difference Fourier syntheses using the software SHELTXL.[29] Structure refinements were made on F^2 by the full-matrix least-squares technique. The non-hydrogen atoms were refined with anisotropic displacement parameters. The hydrogen atoms were placed in their ideal positions but not refined.

Kinetics. The kinetics of the oxidation of NO_2^- by *trans*-$[Ru^{VI}(L)(O)_2]^{2+}$ were studied by using either a Hi-Tech SF-61 stopped-flow spectrophotometer or Hewlett-Packard 8452A diode-array spectrophotometer. The concentrations of NO_2^- were at least in 10-fold excess of that of Ru^{VI}. The reaction progress was monitored by observing absorbance changes at 390 nm (λ_{max} of Ru^{VI}). Pseudo-first-order rate constants, k_{obs}, were obtained by nonlinear least-squares fits of A_t vs t according to the equation $A_t = A_\infty + (A_0 - A_\infty)\exp(-k_{obs}t)$, where A_0 and A_∞ are the initial and final absorbance, respectively. The effects of temperature were studied from 288.0 to 318.0 K, and activation parameters were obtained from the plot of $\ln(k_2/T)$ vs $1/T$ according to the Eyring equation.

Results and Discussion

Synthesis and Characterization of *trans*-$[Ru^{IV}(L)(O)(ONO_2)]^+$ (2). Reaction of *trans*-$[Ru^{VI}(L)(O)_2](ClO_4)_2$ ([**1**]$(ClO_4)_2$) with 1.1 equiv of $NaNO_2$ in H_2O/CH_3CN produces *trans*-$[Ru^{IV}(L)(O)(ONO_2)](ClO_4)$ ([**2**]ClO_4) as a purple solid. [**2**]ClO_4 has a room-temperature magnetic moment of μ_{eff} = 2.97 μ_B (Gouy method), consistent with its formulation as a d^4 Ru^{IV} complex. The IR spectrum (KBr disk) shows peaks at 1275, 1015, and 835 cm^{-1} which are absent in the starting *trans*-$[Ru^{VI}(L)(O)_2](ClO_4)_2$ complex; they are assigned to $\nu_{sym}(NO_2)$, ν(N−O), and ν(Ru=O), respectively. In complexes containing nitrato ligands bound through one oxygen atom, the $\nu_{sym}(NO_2)$ and ν(N−O) occur in the range 1290−1253 and 1034−970 cm^{-1} respectively.[30] In *trans*-$[Ru^{IV}(L)(O)(OH_2)](ClO_4)_2$ ν(Ru=O) occurs at 845 cm^{-1}.[20] These IR assignments are supported by ^{18}O-labeling experiments described below.

The ESI/MS spectrum (+ve mode) of [**2**]ClO_4 in 1 mM CF_3COOH in H_2O/CH_3CN (1:1, v/v)[31] shows the most abundant peak at m/z = 520, $[2]^+$; there is excellent agreement between the experimental and simulated isotopic distribution patterns. This peak gradually decreases with the concomitant appearance of a peak at m/z = 475, which corresponds to $[Ru(L)(O)(OH)]^+$; the same peak also occurs in the spectrum of *trans*-$[Ru^{IV}(L)(O)(OH_2)](ClO_4)_2$. This indicates that the (nitrato)oxoruthenium(IV) species $\mathbf{2}^+$ undergoes aquation, and the half-life is ca. 30

(20) Che, C. M.; Tang, W. T.; Wong, W. T.; Lai, T. F. *J. Am. Chem. Soc.* **1989**, *111*, 9048−9056.
(21) Che. C. M.; Tang, W. T.; Wong, K. Y.; Li, C. K. *J. Chem. Soc., Dalton Trans.* **1991**, 3277−3280.
(22) Che, C. M.; Tang, W. T.; Lee, W. O.; Wong, K. Y.; Lau, T. C. *J. Chem. Soc., Dalton Trans.* **1992**, 1551.
(23) Yiu, D. T. Y.; Lee, M. F. W.; Lam, W. W. Y.; Lau, T. C. *Inorg. Chem.* **2003**, *42*, 1225−1232.
(24) Lam, W. W. Y.; Yiu, S. M.; Yiu, D. T. Y.; Lau, T. C.; Yip, W. P.; Che, C. M. *Inorg. Chem.* **2003**, *42*, 8011−8018.
(25) Yiu, D. T. Y. Chow, K. H.; Lau, T. C. *J. Chem. Soc., Dalton Trans.* **2000**, 17−20.
(26) Armarego, W. L. F.; Perrin, D. D. *Purification of Laboratory Chemicals*, 4th ed.; Reed Educational and Professional Publishing Ltd.: Oxford, U.K., 1996.
(27) *SAINT+*, ver. 6.02a; Bruker Analytical X-ray System, Inc.: Madison, WI, 1998.
(28) Sheldrick, G. M. *SADABS, Empirical Absorption Correction Program*; University of Göttingen: Göttingen, Germany, 1997.
(29) Sheldrick, G. M. *SHELXTL, Reference Manual*, ver. 5.1; Bruker Analytical X-ray System, Inc.: Madison, WI, 1997.
(30) Gatehouse, B. M.; Livingstone, S. E.; Nyholm, R. S. *J. Chem. Soc.* **1957**, 4222−4225

(31) The same mass spectrum was obtained in H_2O/CH_3CN without acid. CH_3CN was added to increase both the solubility of the complex and the electrospraying efficiency.

Scheme 1

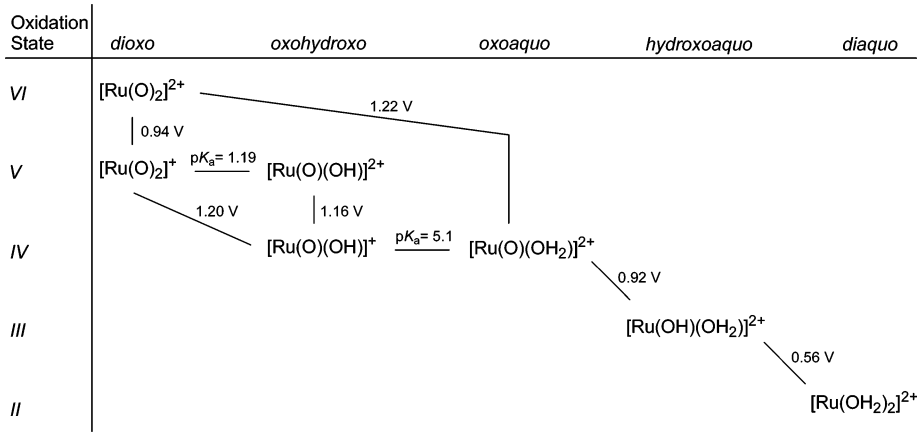

Table 1. Selected Bond Lengths (Å) and Angles (deg) for *trans*-$[Ru^{IV}(L)(O)(ONO_2)]ClO_4$

bond lengths (Å)		bond angles (deg)	
Ru−O(3)	1.735(3)	O(3)−Ru−O(4)	171.19(15)
Ru−O(4)	2.163(4)	O(3)−Ru−O(1)	90.52(12)
Ru−O(1)	2.123(3)	O(3)−Ru−O(2)	87.09(13)
Ru−O(2)	2.171(3)	O(3)−Ru−N(1)	92.64(16)
Ru−N(1)	2.104(4)	O(3)−Ru−N(2)	94.91(15)
Ru−N(2)	2.101(4)	Ru−O(4)−N(3)	138.49(35)
N(3)−O(4)	1.255(6)	O(4)−N(3)−O(5)	121.24(51)
N(3)−O(5)	1.226(8)	O(4)−N(3)−O(6)	118.32(47)
N(3)−O(6)	1.228(7)	O(5)−N(3)−O(6)	120.36(55)

min. at 24 °C. In CH_3CN only the peak at m/z = 520 is observed, which remains unchanged for at least 2 h at room temperature.

X-ray Structure of *trans*-$[Ru^{IV}(L)(O)(ONO_2)]ClO_4$. The structure of [**2**]ClO_4 has been determined by X-ray crystallography (Figure 2). The ruthenium center adopts a distorted octahedral geometry with the oxo and the nitrato ligands trans to each other. The nitrato ligand is O-bonded to the ruthenium center in a monodentate fashion. The Ru=O distance of 1.735(3) Å is similar to that of *trans*-$[Ru^{IV}(L)(O)(OH_2)]^{2+}$ (1.739(2) Å).[20] The Ru−ONO_2 distance is 2.163(4) Å, and the Ru−O(4)−N(3) angle is bent with an angle of 138.46(35)°.

^{18}O-Labeled Study: Reaction of *trans*-$[Ru^{VI}(L)(^{18}O)_2](ClO_4)_2$ with $N^{16}O_2^-$. *trans*-$[Ru^{VI}(L)(^{18}O)_2](ClO_4)_2$ ([**1**-$^{18}O_2$]$(ClO_4)_2$) was prepared in the same way as the ^{16}O analogue using $H_2{}^{18}O$ (95 atom % ^{18}O) as the solvent. The IR spectrum of the compound shows $\nu(^{18}O{=}Ru{=}^{18}O)$ at 834 cm^{-1}, close to the value of 830 cm^{-1} calculated from a simple diatomic harmonic oscillator model using $\nu(^{16}O{=}Ru{=}^{16}O)$ = 873 cm^{-1}. The ESI/MS spectrum (+ve mode) of [**1**-$^{18}O_2$]$(ClO_4)_2$ in 1 mM of CF_3COOH in $H_2{}^{16}O/CH_3CN$ (1:1, v/v)[31] shows peaks at m/z = 239.8 [**1**-$^{18}O_2$]$^{2+}$, 260.7 [**1**-$^{18}O_2$ + CH_3CN]$^{2+}$, 281.3 [**1**-$^{18}O_2$ + $2CH_3CN$]$^{2+}$, 479.1 [Ru(L)(^{18}O)(^{18}OH)]$^+$, and 579.1 [**1**-$^{18}O_2$ + ClO_4]$^+$ (Figure 3). The peak at m/z = 479.1 arises from $[Ru^{IV}(L)(^{18}O)(^{18}OH_2)]^{2+}$ ([M − H]$^+$), which is probably produced by reduction of $[Ru^{VI}(L)(^{18}O)_2]^{2+}$ during the electrospraying process. Analysis of these clusters (except the one centered at m/z = 479.1) shows that they all have the same isotopic composition of 85% **1**-$^{18}O_2$, 15% **1**-$^{18}O^{16}O$, and <1% **1**-$^{16}O_2$ (each ±5%). The isotopic composition of these clusters remains unchanged for over 2 h at 24 °C, indicating that there is no O-exchange between the complex and $H_2{}^{16}O$ during this period. The unlabeled [**1**]$(ClO_4)_2$ exhibits a similar mass spectrum, with the doubly charge peaks 2 m/z units lower and the singly charge peaks 4 m/z units lower.

Reaction of [**1**-$^{18}O_2$]$(ClO_4)_2$ with 1.1 equiv of $N^{16}O_2^-$ in $H_2{}^{16}O/CH_3CN$ (1:1, v/v) readily produces the ^{18}O-enriched (nitrato)oxoruthenium(IV) complex [**2**-$^{18}O_2$]ClO_4. The IR spectrum (Figure 4) shows $\nu_{sym}(NO_2)$ at 1266 cm^{-1} which is broadened and shifted by around −10 cm^{-1} compared to the ^{16}O analogue. There are also additional bands at 990 and 798 cm^{-1} which are assigned to $\nu(N{-}^{18}O)$ and $\nu(Ru{=}^{18}O)$, respectively. These values are in close agreement with the calculated

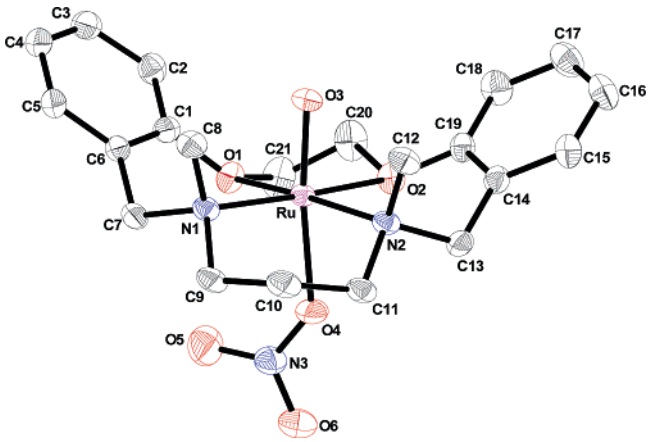

Figure 2. ORTEP of $[Ru^{IV}(L)(O)(ONO_2)]^+$ (**2**$^+$). Thermal ellipsoids are drawn at the 30% probability (hydrogen atoms are omitted for clarity).

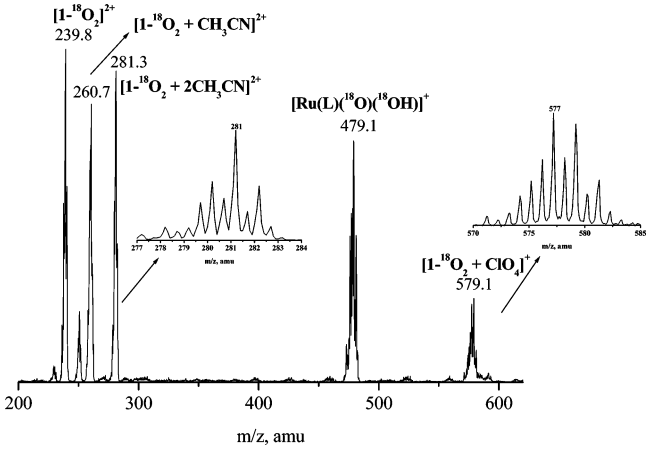

Figure 3. ESI/MS spectrum of *trans*-$[Ru^{VI}(L)(^{18}O)_2](ClO_4)_2$ ([**1**-$^{18}O_2$]$(ClO_4)_2$) in 1 mM CF_3COOH in $H_2{}^{16}O/CH_3CN$ (1:1, v/v).

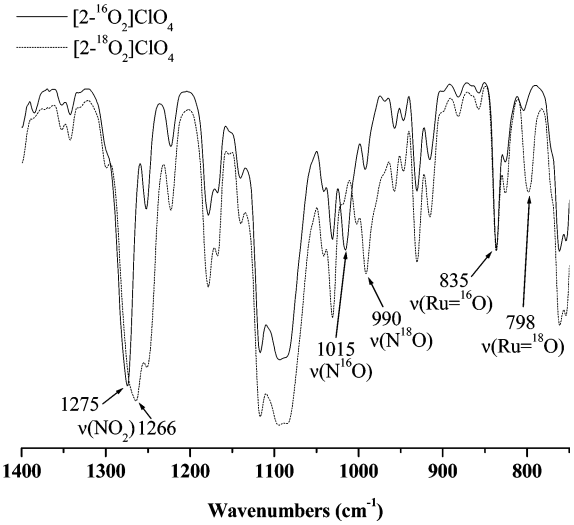

Figure 4. IR spectra (KBr) of [**2**-$^{16}O_2$]ClO_4 and [**2**-$^{18}O_2$]ClO_4 in the range 1400−750 cm^{-1}.

value of 988 and 794 cm^{-1}, respectively. Further evidence of ^{18}O-labeling in the (nitrato)oxoruthenium(IV) complex is obtained from ESI/MS experiments described below.

The ESI/MS spectrum of [**2**-$^{18}O_2$]ClO_4 taken 5 min after dissolution in 1 mM CF_3COOH in H_2O/CH_3CN (1:1, v/v) shows the most abundant peak at $m/z = 524$ [**2**-$^{18}O_2$]$^+$. There is also a smaller peak at $m/z = 477$ which arises from the presence of a small amount of *trans*-[Ru^{IV}(L)(^{18}O)($^{16}OH_2$)]$^{2+}$ ([M − H]$^+$) in the solution. Analysis of the [**2**-$^{18}O_2$]$^+$ cluster (Figure 5) indicates that although there are on the average two ^{18}O atoms/ion; the actual isotopic composition is 30% [**2**-$^{18}O^{16}O$]$^+$, 40% [**2**-$^{18}O_2$]$^+$, and 30% [**2**-$^{18}O_3$]$^+$ (each ±5%). As discussed in more detail below, we propose that this isotopic composition arises from scrambling of the ^{18}O atoms in the initially formed *trans*-[Ru^{IV}(L)(^{18}O)($^{18}ONO_2$)]$^+$ from oxygen atom transfer (eq 2). For random scrambling the % of ions with 0 ^{18}O, 1 ^{18}O, 2 ^{18}O, 3 ^{18}O, and 4 ^{18}O are 6.25, 25, 37.5, 25, and 6.25, respectively, which are in reasonable agreement with the observed values.

$$\textit{trans}\text{-}[Ru^{VI}(L)(^{18}O)_2]^{2+} + NO_2^- \rightarrow \textit{trans}\text{-}[Ru^{IV}(L)(^{18}O)(^{18}ONO_2)]^+ \quad (2)$$

Similar to the ^{16}O analogue, the peak at $m/z = 524$ gradually decreases while the peak at $m/z = 477$ increases (Figure 6), indicating aquation of [**2**-$^{18}O_2$]$^+$ to give *trans*-[Ru^{IV}(L)(^{18}O)($^{16}OH_2$)]$^{2+}$. The $t_{1/2}$ for this aquation is ca. 30 min. at 24 °C. Notably, although the intensities of the two peaks vary with time, the isotopic distributions remain unchanged. This means that there is no O-exchange between [**2**-$^{18}O_2$]$^+$ and $H_2{}^{16}O$ and between the oxo ligand in *trans*-[Ru^{IV}(L)(^{18}O)($^{16}OH_2$)]$^{2+}$ and $H_2{}^{16}O$ during this period (2 h, 24 °C).

The nitrate released during the aquation of [**2**-$^{18}O_2$]$^+$ was shown to be quantitative by ion chromatography. It was also monitored by ESI/MS in the negative mode. Figure 7 shows the ESI/MS spectra (−ve mode) of [**2**-$^{18}O_2$]ClO_4 at various time intervals after dissolution in 1 mM CF_3COOH in H_2O/CH_3CN (1:1, v/v). Notably $N^{16}O_3^-$ ($m/z = 62$), $N^{18}O^{16}O_2^-$ ($m/z = 64$), $N^{18}O_2{}^{16}O^-$ ($m/z = 66$), and $N^{18}O_3^-$ ($m/z = 68$) are all detected. The intensities of all these peaks increase with time, consistent with the release of nitrate during aquation of [**2**-$^{18}O_2$]$^+$. The $t_{1/2}$ is ca. 30 min. at 24 °C, in agreement with the result obtained from monitoring [**2**-$^{18}O_2$]$^+$ in the positive mode. Significantly the *relative* intensities of the four peaks remain more or less unchanged, and assuming that the relative intensities of the peaks are equal to the relative amounts of the respective ions, then the average % of $N^{16}O_3^-$, $N^{18}O^{16}O_2^-$, $N^{18}O_2{}^{16}O^-$, and $N^{18}O_3^-$ = 14, 41, 38, and 7, respectively (each ±5%). If random scrambling of the ^{18}O atoms has occurred in the initially formed *trans*-[Ru^{IV}(L)(^{18}O)($^{18}ONO_2$)]$^+$ prior to aquation, as described for the [**2**-$^{18}O_2$]$^+$ species, then the % should be 12.5, 37.5, 37.5, and 12.5, respectively, which is in reasonable agreement with the observed values. Independent experiments indicate that there is no O-exchange between both $NaNO_3$ and $NaNO_2$ with $H_2{}^{18}O$ under similar conditions.

Kinetic Studies. Figure 8 shows the spectrophotometric changes when a solution of *trans*-[Ru^{VI}(L)$(O)_2$]$^{2+}$ (1.0×10^{-4} M) was mixed with a solution of NO_2^- (4.0×10^{-4} M) at 298.0 K, pH = 1.06, and $I = 0.1$ M. There is an initial rapid reaction ($t_{1/2} \sim 20$ s), followed by a much slower one ($t_{1/2} \sim 30$ min) with relatively small absorbance changes. No clear-cut isosbestic points were observed for both steps. Examination by ESI/MS and UV/vis spectrophotometry shows that the product for the first and second steps are *trans*-[Ru^{IV}(L)(O)-(ONO_2)]$^+$ and *trans*-[Ru^{IV}(L)(O)(OH_2)]$^{2+}$, respectively. Ionic chromatography indicates quantitative formation of NO_3^- after 120 min. Thus, the stoichiometry for the first and second steps can be represented by eqs 3 and 4, respectively. Further reduction of *trans*-[Ru^{IV}(L)(O)(OH_2)]$^{2+}$ was not observed for at least 24 h.

$$\textit{trans}\text{-}[Ru^{VI}(L)(O)_2]^{2+} + NO_2^- \rightarrow \textit{trans}\text{-}[Ru^{IV}(L)(O)(ONO_2)]^+ \quad (3)$$

$$\textit{trans}\text{-}[Ru^{IV}(L)(O)(ONO_2)]^+ + H_2O \rightarrow \textit{trans}\text{-}[Ru^{IV}(L)(O)(OH_2)]^{2+} + NO_3^- \quad (4)$$

The kinetics of the reaction represented by eq 3 were followed at 390 nm under pseudo-first-order conditions ([Ru^{VI}] = $2.5 \times 10^{-5} - 1.0 \times 10^{-4}$ M, [NO_2^-] = $1.0 \times 10^{-3} - 2.0 \times 10^{-2}$ M). The reaction was found to be first order in both [Ru^{VI}] and [NO_2^-]. The second-order rate constant k_2 increases with pH (1−3); a plot of $1/k_2$ versus [H^+] is linear (Figure 9). This is consistent with the relationship shown in eq 5.

$$k_2 = \frac{k}{1 + [H^+]/K_a} \quad (5)$$

K_a is the acid dissociation constant of nitrous acid. A nonlinear least-squares fit of the data to eq 5 (Figure 9) gives $k = (2.33 \pm 0.15) \times 10^4$ M^{-1} s^{-1} and $K_a = (9.10 \pm 0.90) \times 10^{-4}$ M. The value of K_a is in good agreement with the literature value of $K_a = 1.1 \times 10^{-3}$ M.[32]

At pH = 2.92 and $I = 0.1$ M, $\Delta H^{\ddagger}$ and $\Delta S^{\ddagger}$ were found to be 4.2 ± 0.2 kcal mol^{-1} and -26 ± 3 cal mol^{-1} K^{-1}, respectively.

The observed acid dependence of k_2 is consistent with the reaction scheme shown in eqs 6 and 7.

(32) Smith, R. M.; Martell, A. E. *Critical Stability Constants*; Plenum Press: New York, 1976; Vol. 4, p 47.

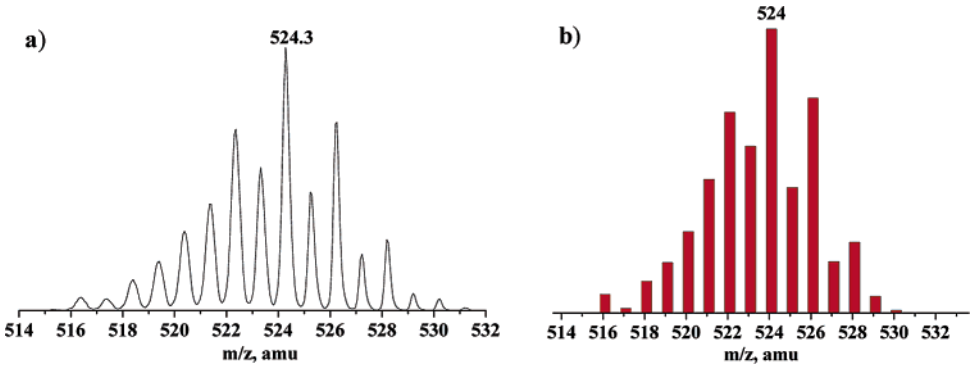

Figure 5. (a) Expanded isotopic distribution of the cluster at $m/z = 524$ in the ESI/MS spectrum of [**2**-$^{18}O_2$]ClO_4. (b) Simulated isotopic pattern for 30% [**2**]-^{18}O, 40% [**2**]-$^{18}O_2$, and 30% [**2**]-$^{18}O_3$.

$$HNO_2 \overset{K_a}{\rightleftharpoons} NO_2^- + H^+ \quad (6)$$

$$trans\text{-}[Ru^{VI}(L)(O)_2]^{2+} + NO_2^- \overset{k}{\rightarrow} trans\text{-}[Ru^{IV}(L)(O)(ONO_2)]^+ \quad (7)$$

The kinetics of the second step (eq 4), which corresponds to aquation of *trans*-$[Ru^{IV}(L)(O)(ONO_2)]^+$, were monitored at 266 nm. The rate constant, k_{aq} was found to be $(3.90 \pm 0.02) \times 10^{-4}$ s^{-1} at 298.0 K, pH = 1.06, $I = 0.1$ M, $[Ru^{IV}] = 1.0 \times 10^{-4}$ M, and $[NO_3^-] = 1.0 \times 10^{-3}$ M. Attempts were also made to study the reverse anation of *trans*-$[Ru^{IV}(L)(O)(OH_2)]^{2+}$ by nitrate. However, addition of excess NO_3^- (0.01 M) to a solution of *trans*-$[Ru^{IV}(L)(O)(OH_2)]^{2+}$ (1×10^{-4} M) at pH = 1.06 did not result in any spectral change for over 5 h at 25 °C, suggesting that the anation rate is very slow.

Mechanism of Nitrite Oxidation by *trans*-$[Ru^{VI}(L)(O)_2]^{2+}$. Reaction of *trans*-$[Ru^{VI}(L)(O)_2]^{2+}$ with nitrite in aqueous solution or in H_2O/CH_3CN produces *trans*-$[Ru^{IV}(L)(O)(ONO_2)]^+$, which then undergoes a relatively slow aquation to give *trans*-$[Ru^{IV}(L)(O)(OH_2)]^{2+}$. These processes have been monitored by both ESI/MS and UV/vis spectrophotometry. The structure of *trans*-$[Ru^{IV}(L)(O)(ONO_2)]^+$ has been determined by X-ray crystallography.

In principle of the oxidation of nitrite by *trans*-$[Ru^{VI}(L)(O)_2]^{2+}$ could occur by an outer-sphere electron-transfer mechanism shown in eqs 8−11.

$$trans\text{-}[Ru^{VI}(O)_2]^{2+} + NO_2^- \rightarrow trans\text{-}[Ru^{V}(L)(O)_2]^+ + NO_2 \quad k \quad (8)$$

$$trans\text{-}[Ru^{V}(L)(O)_2]^+ + 2H^+ + NO_2^- \rightarrow trans\text{-}[Ru^{IV}(L)(O)(OH_2)]^{2+} + NO_2 \quad \text{fast} \quad (9)$$

$$2NO_2 + H_2O \rightarrow NO_2^- + NO_3^- + 2H^+ \quad \text{fast} \quad (10)$$

$$trans\text{-}[Ru^{IV}(L)(O)(OH_2)]^{2+} + NO_3^- \rightarrow trans\text{-}[Ru^{IV}(L)(O)(ONO_2)]^+ \quad (11)$$

In acidic solutions *trans*-$[Ru^{V}(L)(O)_2]^+$ is a stronger oxidant than *trans*-$[Ru^{VI}(O)_2]^{2+}$. The disproportionation reaction of NO_2 is known to be fast, with a rate constant of 1.2×10^7 M^{-1} s^{-1}.[7] Although the above outer-sphere mechanism is consistent with the observed rate law, the oxygen atom required for the conversion of nitrite to nitrate would come from the solvent water. Moreover, the anation reaction by NO_3^- shown in eq 11 is much slower than the observed reaction rate. A comparison of the observed rate constant with the theoretical rate constant for outer-sphere electron transfer also indicates that the outer-sphere mechanism is unlikely. An estimation of the theoretical rate constant for outer-sphere electron transfer (k_{12}) can be made

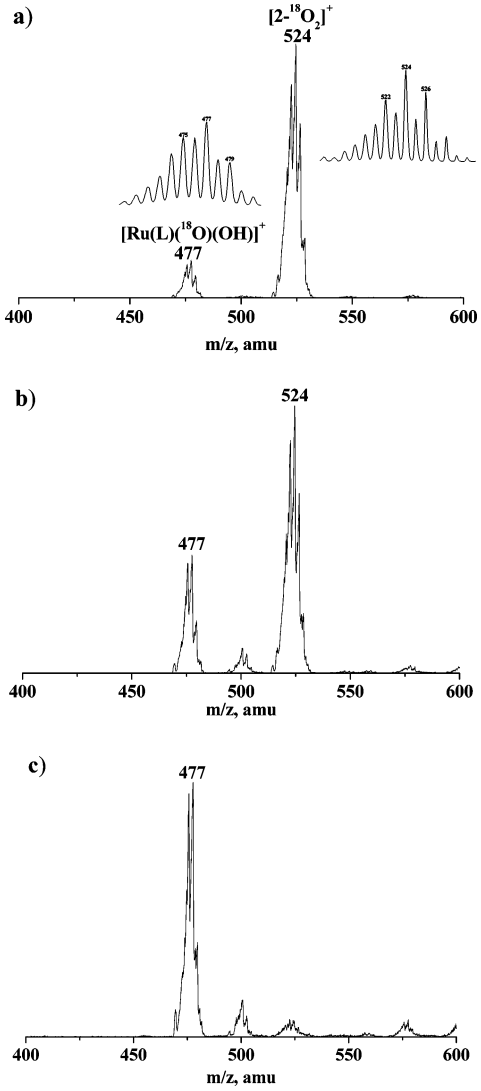

Figure 6. ESI/MS spectra (+ve mode) of [**2**-$^{18}O_2$]ClO_4 in 1 mM CF_3COOH/CH_3CN (1:1, v/v) at different time intervals: (a) 5 min; (b) 30 min; (c) 120 min. (Insets show the expanded isotopic patterns.)

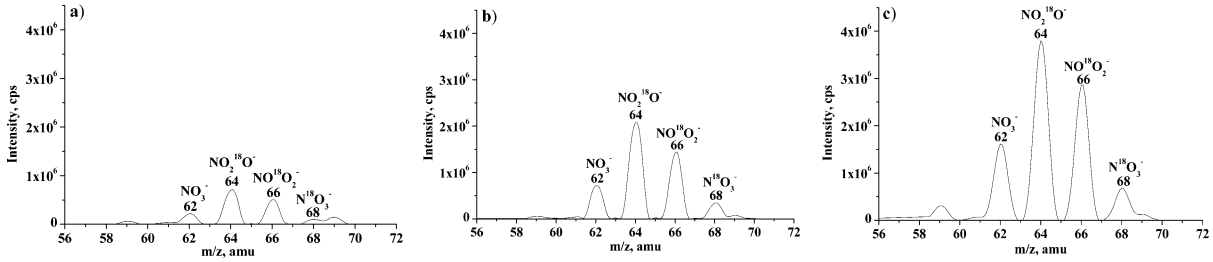

Figure 7. ESI/MS spectra (−ve mode) of [**2**-$^{18}O_2$]ClO_4 in 1 mM of CF_3COOH in H_2O/CH_3CN (1:1, v/v) at different time intervals: (a) 5 min; (b) 30 min; (c) 120 min.

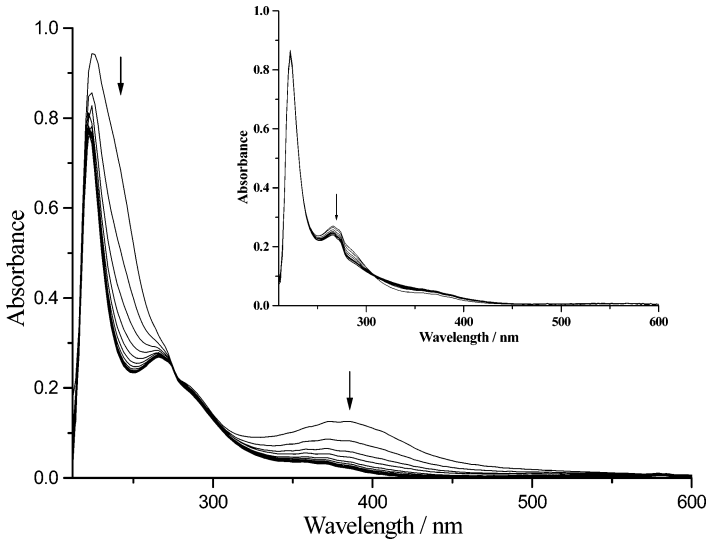

Figure 8. Spectrophotometric changes at 20 s intervals for the oxidation of NO_2^- (4.0×10^{-4} M) by *trans*-[Ru^{VI}(L)$(O)_2$]$^{2+}$ (1.0×10^{-4} M) at 298.0 K, pH = 1.06, and $I = 0.1$ M. The inset shows the spectrophotometric changes at 1200 s intervals for the second step.

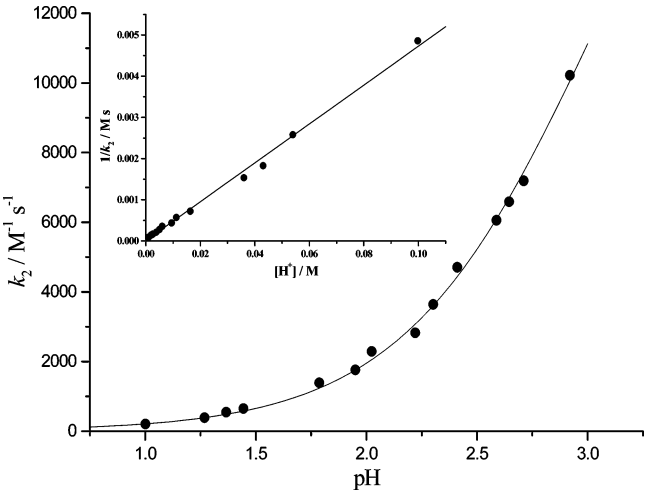

Figure 9. Plot of k_2 vs pH for the oxidation of nitrite by *trans*-[Ru^{VI}(L)-$(O)_2$]$^{2+}$ (1.0×10^{-4} M) at 298.0 K. The inset shows the corresponding plot of $1/k_2$ vs [H^+] (slope = $(4.72 \pm 0.09) \times 10^{-2}$, *y*-intercept = $(6.79 \pm 0.34) \times 10^{-6}$, $r = 0.998$).

by using the Marcus cross-relation,[33] eqs 12 and 13 (neglecting work terms):

$$k_{12} = (k_{11}k_{22}K_{12}f_{12})^{1/2} \tag{12}$$

$$\log f_{12} = \frac{(\log K_{12})^2}{4\log(k_{11}k_{22}/10^{22})} \tag{13}$$

K_{12}, the equilibrium constant for the reaction, is calculated from the reduction potentials for the [Ru^{VI}(L)$(O)_2$]$^{2+}$/[Ru^{V}(L)$(O)_2$]$^+$ (0.94 V vs NHE)[20] and the NO_2/NO_2^- (1.04 V)[34] couples. A value of 1×10^5 M^{-1} s^{-1} is used for k_{11}, the self-exchange rate for [Ru^{VI}(L)$(O)_2$]$^{2+}$/[Ru^{V}(L)$(O)_2$]$^+$;[35] k_{22}, the self-exchange rate for NO_2/NO_2^-, is taken as 0.3 M^{-1} s^{-1}.[7] Using these data, k_{12} is calculated to be 2.4×10 M^{-1} s^{-1} at 298 K, which is almost 3 orders of magnitude slower than the experimental rate constant ($k = 2.33 \times 10^4$ M^{-1} s^{-1}).

On the other hand, all the results are consistent with an oxygen atom transfer mechanism. The ^{18}O-enriched (nitrato)-oxoruthenium(IV) species [**2**-$^{18}O_2$]ClO_4 is readily formed from reaction of [**1**-$^{18}O_2$]$(ClO_4)_2$ and $N^{16}O_2^-$. The IR spectrum shows the expected shift of ν(N−O) upon ^{18}O-labeling, which is consistent with direct oxygen atom transfer. Analysis of the ESI/MS spectra of [**2**-$^{18}O_2$]ClO_4 and the nitrate released from this species during aquation indicates that ^{18}O-scrambling has occurred. A reversible oxygen-atom transfer mechanism is proposed to account for the scrambling of the ^{18}O atoms, as shown in Scheme 2.

The proposed mechanism starts with oxygen-atom transfer to produce initially *trans*-[Ru^{IV}(L)$(^{18}O)(^{18}ONO_2)$]$^+$ as shown

(33) Marcus, R. A.; Eyring, H. *Annu. Rev. Phys. Chem.* **1964**, *15*, 155−196.
(34) Ram, M. S.; Stanbury, D. M. *Inorg. Chem.* **1985**, *24*, 2954−2962.
(35) Li, C. K. Ph.D. Thesis, University of Hong Kong, 1991.

Scheme 2

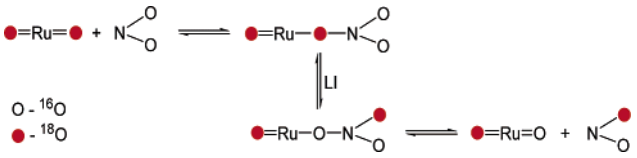

in eq 2. This species then undergoes rapid linkage isomerization (LI) through rotation of the nitrato ligand. This is followed by back oxygen-atom transfer to generate singly ^{18}O-labeled *trans*-$[Ru^{VI}(L)(^{18}O)(^{16}O)]^{2+}$ and $N^{18}O^{16}O^-$ ions. Repetition of these processes would result in the observed scrambling of the ^{18}O atoms in the (nitrato)oxoruthenium(VI) species. Reversible N−O photocleavage of bound nitrite in chromium macrocyclic amine complexes has been observed previously.[36] In the present case the reaction is not light-induced, since the same results were obtained by carrying out the reaction in the dark or in normal room light.

Conclusions

Reaction of *trans*-$[Ru^{VI}(L)(O)_2]^{2+}$ with nitrite in aqueous solution or in H_2O/CH_3CN produces *trans*-$[Ru^{IV}(L)(O)(ONO_2)]^+$, which then undergoes relatively slow aquation to give *trans*-$[Ru^{IV}(L)(O)(OH_2)]^{2+}$. Results of kinetic and ^{18}O-labeling studies are consistent with direct oxygen atom transfer from ruthenium(VI) to nitrite. Scrambling of oxygen atoms is observed in the nitrato(oxo)ruthenium(IV) species. This can be accounted for by a mechanism that involves linkage isomerization of the nitrato ligand and reversible oxygen atom transfer. This is the first definitive example of oxygen atom transfer from a metal−oxo species to nitrite.

Acknowledgment. The work described in this paper was supported by the Research Grants Council of Hong Kong (Grant CityU 1105/02P) and the City University of Hong Kong (Grant 7001582).

Supporting Information Available: A table of rate data and IR, ESI/MS, and UV/vis spectra. This material is available free of charge via the Internet at http://pubs.acs.org.

JA064975G

(36) DeRossa, F.; Bu, X.; Ford, P. C. *Inorg. Chem*. **2005**, *44*, 4157−4165.